Title

Regulation and localization of vascular endothelial growth factor within the mammary glands during the transition from late gestation to lactation

Journal

Domestic Animal Endocrinology, 54

ISSN

0739-7240

Authors

VanKlompenberg, MK

Manjarín, R

Donovan, CE

et al.

Publication Date

2016

DOI

10.1016/j.domaniend.2015.09.003

Peer reviewed

Regulation and localization of vascular endothelial growth factor within the mammary glands during the transition from late gestation to lactation

M.K. VanKlompenberg, R. Manjarín, C.E. Donovan, J.F. Trott and R.C. Hovey

Department of Animal Science, University of California Davis, Davis, CA

Corresponding author: R.C. Hovey, rchovey@ucdavis.edu. 2145 Meyer Hall, One Shields Avenue, University of California Davis, Davis CA 95616.

Abstract

The vascular network within the developing mammary gland (MG) grows in concert with the epithelium to prepare for lactation, although the mechanisms coordinating this vascular development are unresolved. Vascular endothelial growth factor A (VEGF-A) mediates angiogenesis and vascular permeability in the MG during pregnancy and lactation, where its expression is upregulated by prolactin. Given our previous finding that late-gestational hyperprolactinemia induced by domperidone (DOM) increased subsequent milk yield from gilts, we sought to establish changes in vascular development during late gestation and lactation in the mammary glands of these pigs as well as determine whether DOM altered MG angiogenesis and the factors regulating it. Gilts received either no treatment (n=6) or DOM (n=6) during late gestation, then had their MG biopsied from late gestation through lactation to assess microvessel density, VEGF-A distribution and mRNA expression, and aquaporin (AQP) gene expression. Microvessel density in the MG was unchanged during gestation then increased between days 2 and 21 of lactation ($P < 0.05$). The local expression of mRNA for *VEGF-A*$_{120}$, *VEGF-A*$_{147}$, *VEGF-A*$_{164}$, *VEGF-A*$_{164}$*b*, *VEGF-A*$_{188}$, *VEGF receptors-1* and *-2*, and *AQP1* and *AQP3* all generally increased during the transition from gestation to lactation ($P < 0.05$). Immunostaining localized VEGF-A to the apical cytoplasm of secretory epithelial cells, consistent with a far greater concentration of VEGF-A in colostrum/milk versus plasma ($P < 0.0001$). There was no effect of DOM on any of the variables analyzed. In summary, we find that vascular development in the MG increases during lactation in first-parity gilts and that VEGF-A is a part of the mammary secretome. Although late gestational hyperprolactinemia increases milk yield, there was no evidence it altered vascular development.

Keywords: angiogenesis; mammary gland; pig; vascular endothelial growth factor A; prolactin

1. Introduction

Successful lactation relies on the coordinated processes of mammary epithelial growth and differentiation during gestation [1] that occur in close apposition to a complex vascular network [2]. This network forms throughout gestation via angiogenesis [3] to ultimately provide sufficient blood flow and the associated nutrients required for milk production [4]. A potent initiator of angiogenesis in all mammalian organs is vascular endothelial growth factor-A (VEGF-A; [5]). This locally-produced factor is critical for complete mammary gland (MG) development, where the conditional deletion of VEGF-A in the mammary myoepithelium and epithelium of mice decreased blood vessel density and function, and severely impacted milk production and pup growth [6]. Additionally, VEGF-A regulates vascular permeability [5] that is essential for the regulated transfer of nutrients, oxygen, and metabolic waste during milk synthesis and secretion [7].

Various factors modulate the expression and actions of VEGF-A and hence may alter angiogenesis and vascular permeability within the MG. The effects of VEGF-A are conferred via two tyrosine kinase receptors, VEGF-receptors-1 and -2 (VEGFR-1 and VEGFR-2; [8]) that can have their effects enhanced by the co-receptor neuropilin 1 (NP1; [9]). Furthermore, there is considerable potential for hypoxia to occur within the MG during gestation and lactation given the increased growth and metabolic rate of mammary epithelial cells (MEC; [10]). As a result, increased abundance of hypoxia inducible factor-1α (HIF-1α) can upregulate VEGF-A expression [11, 12]. Finally, sufficient vascular permeability within the MG is realized by the actions of developmentally-regulated [13], water-permeable aquaporins (AQP) that allow water

to move from the microcirculation into milk [14]. Within the mammary glands, AQP1 localizes to the endothelium whereas AQP3 localizes to the epithelium to contribute to milk synthesis [15, 16].

The endocrine system that directs growth and differentiation of the mammary epithelium may also regulate angiogenesis within the MG [17]. Prolactin (PRL) directs the growth and differentiation of MEC during gestation in preparation for lactation [18, 19], and it has been established that the MG of pigs are critically-sensitive to PRL between days 90 and 110 of gestation [20]. As an extension of those findings, we recently used the dopamine type-2 receptor antagonist domperidone (DOM) to induce hyperprolactinemia in late-gestation gilts (average of 51.68 ± 9.2 ng/mL PRL at days 91 and 96 of gestation versus 10.6 ± 1.2 ng/mL, [21]) that resulted in DOM-treated gilts producing significantly more milk during the subsequent lactation. Since PRL also increases the production of VEGF-A by mouse MEC *in vitro* [22], the question arises as to whether the galactopoietic effect of late-gestational hyperprolactinemia is mediated by increased angiogenesis within the MG.

A resolution of the mechanisms underlying the regulation of lactation in sows is warranted given that insufficient milk yield can limit the growth of piglets [23] while galactogogues such as DOM are often used to support human lactation, where the MG of pigs constitutes an authentic model for the breast [24]. Given these considerations, our objective was to investigate whether DOM-induced hyperprolactinemia in first-parity gilts altered various aspects of angiogenesis in their MG. Because we previously showed that late-gestational hyperprolactinemia significantly increased subsequent milk production [21] and milk yield is proportional to mammary blood flow [7], we hypothesized that late gestational

hyperprolactinemia would also promote angiogenesis and the expression of its regulatory factors within the MG.

2. Materials and methods

2.1 Animals and sample collection

All procedures were approved by the University of California, Davis Animal Care and Use Committee (Protocol #15217). In a previously-described study [21], 12 first-parity Yorkshire × Hampshire gilts in two experimental blocks (three gilts per treatment per block) were randomly assigned to receive either no supplement (CON, n=6) or domperidone (DOM, n=6) from days 90 to 110 of gestation. Domperidone-treated gilts received Equidone (11% w/v DOM, 0.4 mg/kg body weight, Equi-tox Pharma, Central, SC, USA) twice-daily in their feed from days 90 to 110 of gestation, where complete intake was confirmed at each feeding. Animals were fed at 0800 and 2000 h and had *ad libitum* access to water via nipple. Gilts were individually housed in 3×3 m pens and moved to farrowing crates on day 111 of gestation. Lactating gilts nursed and weaned standardized litters of approximately the same size (n = 8.37 ± 0.16 piglets).

Mammary glands were biopsied using a vacuum assisted approach [25] on days 90, 100, and 110 of gestation and days 2 and 21 of lactation. For a given time point, biopsies were taken from the same MG in all animals, with gland position across time following a sequential pattern starting from the right posterior gland of the mammary chain, then moving contralateral and thereafter diagonally forward. Each gland was only biopsied once, and only lactating glands that were actively nursed were biopsied. Two or three tissue cores were collected at each biopsy,

where one or two were flash frozen and stored at -80^{o} C while one was fixed in 10% formalin overnight at 4°C.

Blood samples were collected by jugular venipuncture on days 90, 100, and 110 of gestation to confirm hyperprolactinemia as described [21]. Blood samples were also collected from 6 gilts from one experimental block (n=3 CON and n=3 DOM) on days 2 and 21 of lactation. Samples were collected into sodium heparin-coated Vacutainer® tubes (10 mL; BD, Franklin Lakes, NJ, USA) at 0800 h before the feeding (12 h post-DOM ingestion). Plasma was collected after centrifugation at 3,700 × *g* for 15 min at room temperature, aliquoted, and stored at -20°C.

Corresponding colostrum/milk samples were also collected from these same six gilts on days 1 and 20 of lactation. Samples on day 1 were collected approximately 2 h after farrowing. On day 20 of lactation, gilts were given oxytocin (20 IU IM; VetOne, Boise, ID, USA) approximately 1 h after the morning feeding to induce milk ejection. Each milk sample was a composite sample from the anterior, middle, and posterior suckled glands. Samples were collected into 15 mL conical tubes and immediately frozen at -20°C. The skim fraction was obtained following centrifugation at 3,500 × *g* for 10 min at room temperature.

2.2 Immunohistochemistry

2.2.1 Microvessel density. Mammary tissues were processed to paraffin followed by sectioning (5 µm). Sections were deparaffinized in xylene and rehydrated through graded ethanols before permeabilization using 0.3% Triton-X (Promega, Madison WI, USA). Antigen retrieval was performed in citrate buffer (pH 6.0, 45 min, Diagnostic Biosystems, Pleasanton, CA, USA) in a vegetable steamer. Endogenous peroxidases were blocked with 3% hydrogen peroxide, and

endogenous biotin was blocked with a commercial avidin/biotin blocking kit (Vector Laboratories, Burlingame, CA, USA). Blocking was achieved using 10% horse serum for 1 h at room temperature. The primary antibody against CD31 (PECAM-1, 1:200, Millipore, Billerica, MA, USA, #04-1074) was incubated overnight at 4^{o} C. The secondary antibody (biotinylated donkey anti-rabbit, 1:1000, #711-065-152, Jackson ImmunoResearch Laboratories, West Grove, PA, USA) was incubated at room temperature for 45 min followed by 30 min with horseradish peroxidase-conjugated streptavidin (Invitrogen, Grand Island, NY, USA). Immunocomplexes were detected with a 3,3'-diaminobenzidine tetrahydrochloride substrate kit (Invitrogen) and sections counterstained with hematoxylin. Each immunohistochemistry (IHC) run included samples from all timepoints from one CON and one DOM animal as well as a section from the same positive control paraffin block, and a no primary antibody control.

Five independent fields from each section were imaged and analyzed by an observer blinded to treatment using the tracing tool and manual tag function in Image-Pro Express 6.3 (Media Cybernetics, Rockville, MD, USA). Intralobular stromal area was calculated by subtracting the area of all individual alveoli from the area of the lobular region to determine the area of intralobular stroma in μm^2. Microvessel density was then expressed as the number of CD31 positive vessel sections per unit of intralobular stroma area.

2.2.2 Vascular endothelial growth factor A. Immunolocalization of VEGF-A was performed using the above protocol with modifications. Antigen retrieval was performed in citrate buffer in a vegetable steamer for 5 min followed by 10 min on ice. Blocking was achieved using 3% BSA in PBS + 0.05% Tween. An antibody that detects all VEGF-A isoforms (α-VEGF, 1:100, Santa Cruz Biotechnology, Santa Cruz, CA, USA, # sc-152) was incubated overnight at 4^{o} C. This

antibody was shown to detect VEGF-A in the lactating mouse MG, as we have described previously [26], and lactating mouse mammary tissue was used as the positive control for VEGF-A IHC runs. Immunocomplexes were detected using Vector SG chromogen (Vector Laboratories) with a nuclear fast red counterstain (Ricca Chemical Company, Arlington, TX, USA). Each IHC run included all animals at a specific timepoint. Consistency between runs was confirmed using control slides that contained one positive control section from the same paraffin block and one section that was incubated with secondary antibody only. Three independent fields per section were imaged by an observer blinded to treatment so as to define the patterns of VEGF-A localization.

2.3 ELISA for VEGF

The concentration of total VEGF in plasma (days 2 and 21 of lactation) and colostrum/milk samples (days 1 and 20 of lactation) from CON (n=3) and DOM (n=3) gilts was measured by ELISA using a commercial kit (Quantikine Human VEGF, R&D Systems, Minneapolis, MN, USA) that cross-reacts with porcine VEGF [27-29]. A test of parallelism was also conducted where the serial dilution curve was compared to serial dilution curves containing either milk or plasma spiked with VEGF to evaluate potential analyte interference. Samples of skim milk were diluted 100-fold with calibrator diluent whereas plasma samples were undiluted. All samples and standards were analyzed in duplicate. Intra-assay precision for plasma and milk was 4.7% and 12.4%, respectively.

2.4 RNA extraction, cDNA synthesis, and quantitative PCR (qPCR)

Total RNA was extracted using Qiazol (Qiagen, Valencia, CA, USA) according to the manufacturer's instructions. The quantity and quality of RNA was assessed using an ND-1000

spectrophotometer (NanoDrop Technologies, Wilmington, DE, USA) and formaldehyde-agarose gel electrophoresis, respectively. Total RNA was treated with DNAse I (Roche, Indianapolis, IN, USA) and reverse transcribed using random hexamers (2 ng/mL, Amersham Pharmacia Biotech, Inc., Piscataway, NJ, USA), dNTPs (0.4mM, Promega), oligo dT (200 ng/µL, New England Biolabs, Ipswich, MA, USA), RNAse inhibitor (1 U/mL, Stop Rnase Inhibitor, 5 Prime Inc., Gaithersburg, MD, USA) and Moloney Murine Leukemia Virus Reverse Transcriptase (4 U / mL, Promega) for 90 min at 37^{o}C followed by 95^{o}C for 5 min.

Primer sequences for target genes and their annealing temperatures are presented in Tables 1 and 2. Primers were designed to specifically amplify only one splice variant, and all PCR products were cloned into pCR2.1 TOPO (Life Technologies, Carlsbad, CA) and sequence-verified. A relative standard curve was used for all primer sets except *pVEGFA$_{164}$b* to determine the efficiency of each primer pair and to correct for differences in reaction efficiency between plates [30, 31]. We used at least a 5-point standard curve (4-fold or 5-fold serial dilutions) created from cDNA synthesized from RNA extracted from the MG of a sow at d 21 of lactation. The splice variant *pVEGFA$_{164}$b* mRNA was not expressed at sufficient abundance in any tissues to enable the use of cDNA as a standard curve. Instead, plasmid containing the cloned PCR amplicon for *pVEGFA$_{164}$b* was spiked into mouse cDNA to create a 7-point standard curve containing 10-fold dilutions of *pVEGFA$_{164}$b* plasmid template. Non-template and non-reverse transcriptase enzyme negative controls were included in all qPCR plates. Each gene was analyzed in duplicate using 0.2 µL, 0.4 µL or 0.9 µL of cDNA with Fast SYBR® Green Master Mix (Applied Biosystems, Foster City, CA, USA) and 200 nM of each primer. Reactions were heated to 95° C for 20 s followed by 40 cycles of 95 $^{\circ}$C for 3 s and 60 - 64°C for 30 s followed by

194 the generation of a dissociation curve (ABI 7500 Fast Sequence Detection System; Applied
195 Biosystems). Data were analyzed with the 7500 RQ Sequence Detection Systems Software
196 (version 2.0.5, Applied Biosystems). Relative abundance of mRNA was normalized using the
197 geometric mean of three reference genes as previously described (apoptosis inhibitor 5**,**
198 mitochondrial ribosomal protein L39, and vesicle-associated membrane associated protein B/C;
199 [21]).

200 *2.5 Statistical analysis*

201 Data for ELISA in the form of linearized optical densities of the serial dilution curve and
202 serial dilution curves containing either milk or plasma were evaluated for potential interactions
203 by two-way factorial ANOVA (PROC GLM; SAS Institute Inc., Cary, NC), with factors of serial
204 dilution curve type (standard, spiked milk, or spiked plasma) and VEGF concentration in each
205 serial dilution (0, 62.5, 250, 500, or 1000 pg/mL). Comparisons of VEGF concentrations in
206 sample milk and plasma were power transformed to meet normality requirements. Treatment,
207 time of sample collection, and sample type (milk, plasma) were fixed effects. Analyses of all
208 other study parameters were performed using a two-way ANOVA linear mixed model with
209 repeated measurements in SAS using the PROC MIXED platform. Treatment, time and their
210 interaction were fixed effects, while sow was nested in block as a random effect, and sow was
211 nested in treatment as a repeated measure. Autoregressive (AR(1); SAS) was used as the
212 covariate structure. Normality of the residuals and presence of outliers was assessed by SAS
213 (PROC UNIVARIATE) using the Shapiro-Wilk test, Q-Q-plot and externally studentized
214 residuals. When necessary, data was either power transformed by a parameter φ whose optimal
215 value was estimated using the maximum likelihood (ML) method [32], or transformed using the

transreg procedure of SAS and a Box-Cox power transformation. Preplanned means comparisons of main effects and their interactions were performed by orthogonal contrasts using the estimate statement in SAS. Polynomial coefficients to assess linear and quadratic time effects in the response variables were generated using PROC IML in SAS. Pairwise comparisons between least square means were analyzed by Student's t-test. Effects were considered significant at $P < 0.05$ and trends at $P < 0.1$.

3. Results

Vascular development within the MG was assessed as microvessel density using IHC for CD31 (Figure 1). In all pigs the density of microvessels increased linearly from day 90 of gestation to day 21 of lactation ($P < 0.001$). Moreover, the number of vessels in the intralobular stroma was significantly greater at day 21 of lactation compared to day 2 ($P < 0.05$). While we hypothesized that hyperprolactinemic females would have increased vascular development within the mammary glands, DOM treatment did not alter microvessel density in the intralobular stroma during either the treatment window or the subsequent lactation (Figure 1).

Changes in the microvasculature are regulated locally by factors including VEGF-A. There was a significant effect of stage of development on gene expression for *VEGF-A*$_{120}$, *VEGF-A*$_{147}$, *VEGF-A*$_{164}$, *VEGF-A*$_{164}$*b*, and *VEGF-A*$_{188}$ in the MG (Figure 2). Expression of mRNA encoding each of these *VEGF* isoforms increased linearly between day 90 of gestation and day 21 of lactation ($P < 0.001$). In addition, there was a significant quadratic component for the temporal expression of *VEGF-A*$_{188}$ between day 90 of gestation and day 21 of lactation ($P <$

0.001). Gene expression for *VEGF-A*$_{164}$*b* was greater at day 100 compared to day 90 of gestation ($P < 0.05$), while expression of *VEGF-A*$_{120}$, *VEGF-A*$_{147}$, *VEGF-A*$_{164,}$ *VEGF-A*$_{164}$*b* and *VEGF-A*$_{188}$ mRNA was greater at day 2 of lactation compared to day 110 of gestation ($P < 0.05$). Expression of both *VEGF-A*$_{120}$ and *VEGF-A*$_{188}$ mRNA increased further between days 2 and 21 of lactation ($P < 0.01$). Expression of *VEGF-A*$_{205}$ mRNA was not quantified because it was below the level of detectability. By contrast, there was no effect of DOM treatment on *VEGF-A* gene expression at any of the stages examined. However, there was a trend towards a treatment effect for *VEGF-A*$_{120}$ at day 110 of gestation ($P = 0.06$).

To extend our findings regarding the local synthesis of VEGF-A in the MG, we measured its concentrations in colostrum/milk and plasma samples collected on adjacent days from three CON and three DOM gilts. A test of parallelism for the ELISA showed no significant interactions ($P = 0.4518$) between sample type (standard, spiked milk, or spiked plasma) and serial dilutions of the VEGF standard (0, 62,5, 250, 500, and 1000 pg/mL), confirming there was no interference by either analyte. The concentration of VEGF-A was significantly greater in colostrum (mean 39,258 pg/mL) compared to plasma (mean 6.91 pg/mL) during early lactation ($P < 0.0001$; Figure 3), and also in milk (mean 30,320 pg/mL) compared to plasma (mean 5.89 pg/mL) during late lactation ($P < 0.0001$). There was no significant effect of DOM on VEGF concentrations, but there was a numerical treatment effect on VEGF concentrations in plasma ($P = 0.09$). There were no differences in the concentrations of VEGF-A in plasma between days 2 and 21 of lactation, or in colostrum/milk between days 1 and 20 of lactation.

Given the high concentrations of VEGF-A in milk, we immunolocalized VEGF-A within the MG (Figure 4). Distribution of VEGF-A on day 90 of gestation was most evident in denser

alveoli, while the expression of VEGF-A on days 100 and 110 of gestation was relatively homogenous within MEC that were showing overt signs of lactogenesis. By day 2 of lactation the distribution of VEGF was mostly homogeneous throughout the epithelium, with occasional evidence of apical cytoplasmic staining. This apical localization was far more pronounced at day 21 of lactation. Immunoreactivity for VEGF-A was also detected in the alveolar lumenae on days 2 and 21 of lactation. There was no discernible effect of DOM on VEGF abundance or localization.

The effects of VEGF-A are realized through two different tyrosine kinase receptors, VEGFR-1 and VEGFR-2. Expression of the genes encoding VEGFR-1 and VEGFR-2 increased linearly ($P < 0.01$) between day 90 of gestation and day 21 of lactation, and expression of both genes was greater at day 2 of lactation compared to day 110 of gestation ($P < 0.05$; Figure 5). There was no effect of DOM on expression for either of these two receptors at any time. Finally, expression of the VEGF co-receptor *NP1* decreased linearly in both groups between day 90 of gestation and day 21 of lactation ($P < 0.0001$). There was no significant effect of DOM on *NP1* expression (Figure 5). However, a non-significant trend towards a negative effect of DOM on *NP1* expression was evident at day 2 of lactation ($P = 0.06$).

Because angiogenesis may be initiated in response to hypoxia, we examined expression of *HIF-1α* mRNA that increases in this state. Despite these associations, expression of *HIF-1α* did not differ due to treatment or time (data not shown). Lastly, given that VEGF can alter vascular permeability, we quantified expression of two different membrane bound water channels, AQP1 and AQP3 (Figure 6). Expression of *AQP1* increased in a quadratic fashion between day 90 of gestation and day 21 of lactation ($P < 0.05$), where expression was greater at

day 110 of gestation compared to day 100 ($P < 0.05$), and lower ($P < 0.01$) at day 21 of lactation compared to day 2. Meanwhile, expression of *AQP3* increased linearly between day 90 of gestation and day 21 of lactation ($P < 0.0001$) and was greater at day 2 of lactation compared to day 110 of gestation ($P < 0.001$). There was no effect of DOM on either *AQP1* or *AQP3* at any time point.

4. Discussion

To date there has been limited investigation of the regulation of angiogenesis or vascular permeability in the MG during normal growth and development, or the factors regulating these processes. A key promoter of angiogenesis and vascular permeability is VEGF-A [5, 12, 33]. The capillary network within the MG of mice expands during the transition from gestation to lactation, coincident with increased local expression of *VEGF-A* [26, 34]. Here we recorded similar changes in *VEGF-A* gene expression in the MG of pigs as well as for the temporal regulation of VEGFR-1 and VEGFR-2 mRNAs. These findings are consistent with those from mice, where expression of both receptors increased from late gestation to early lactation [26]. A notable distinction was for the expression of *VEGF-A*$_{188}$ mRNA that increased linearly in the MG of pigs between gestation and lactation, whereas in mice it decreased during gestation, then was nearly undetectable during lactation [26]. This contrast may reflect differences in the histomorphology [24] and epithelial-stromal composition [35] of the MG between pigs and mice, where we previously showed that *VEGF-A*$_{188}$ mRNA is synthesized primarily by adipocytes that are far more abundant in the murine MG than in species such as pigs and other livestock [35, 36].

Interestingly, *NP1* expression in the MG declined during lactation at the same time that *VEGFR* expression increased, where cooperativity between these receptors and their relative abundance can modulate VEGF action and angiogenesis [37], arteriogenesis [38] and lymphangiogenesis [39]. Furthermore, NP1 and VEGFR2 can interact across different cell types [40]. Given the intimate and complex relationships between the vasculature, lymphatics, and epithelium during lactation, this finding warrants further investigation with respect to how it contributes to the local regulation of milk synthesis.

Previous studies have implicated PRL in the regulation of angiogenesis in the MG [41, 42] where PRL induces the transcription of *VEGF-A in vitro* [22]. Here we did not find any effect of late-gestational hyperprolactinemia on *VEGF-A* mRNA expression in the MG of pigs, although there was a trend towards a positive effect of DOM on the expression of *VEGF-A*$_{120}$ mRNA on day 110 of gestation. One consideration that may explain the lack of a pronounced positive effect of DOM on *VEGF-A* expression is that late-gestation CON gilts may have already had sufficient concentrations of PRL to induce maximal *VEGF-A* transcription within the MG, given that low concentrations of PRL can induce marked expression of *VEGF-A* mRNA *in vitro* [22].

Our findings also highlight that VEGF-A comprises part of the MG secretome as evidenced from its immunohistochemical localization in secretory MEC and in the luminae of alveoli, and also by increased concentrations of VEGF-A in colostrum and milk compared to plasma. Consistent with our data in pigs, the concentration of VEGF-A in human milk is significantly greater than in the maternal serum [43, 44] and present at similar concentrations to

what we measured in porcine milk. Although we collected colostrum/milk samples 24 h before the corresponding plasma samples, there was no difference in the concentration of VEGF-A in either milk or plasma between early and late lactation, suggesting that the 24 h interval did not affect these findings. While the specific role of milk-borne VEGF-A is not clear, one suggestion is that it may be destined to act on the neonatal gastrointestinal tract to facilitate nutrient uptake [44, 45], where luminal epithelial cells express VEGFR-1 and -2 on their apical membrane [44, 46]. Although DOM treatment did not change the concentration of VEGF in colostrum or milk, this outcome may be due to a small sample size; thus, further investigation is warranted. However, given that DOM treatment increased the production of milk and its consumption by piglets [21], total intake of VEGF by the nursing offspring was increased. Taken together these data suggest that VEGF-A could be an additional factor in milk that may help to promote rapid growth and differentiation of the infant gut [47-51].

Total blood flow, vascular density and permeability can all influence milk production [4, 7]. While the density of capillaries in the mouse MG remains relatively constant through lactation [34], we established that the density of microvessels within the intralobular stroma of the MG in pigs increased throughout lactation, potentially as the result of increased local *VEGF-A*, *VEGFR-1*, and/or *VEGFR-2* gene expression. We also find that gene expression for *AQP1* and *3*, both of which are measures of vascular permeability [52], increases from late gestation to lactation. Nazemi *et al*. [13] also recently reported that expression of *AQP1* and *3 in the MG* of rats increases between gestation and early lactation. Those authors found that *AQP1* expression remained elevated from early to peak lactation, whereas we found that *AQP1* expression in the MG decreased during this period. We also found that *AQP3* expression remained elevated from

day 2 to day 21 of lactation, whereas Nazemi *et al.* [13] found that *AQP3* expression decreased from early to peak lactation. Whether these differences reflect between-species or experimental divergence is unknown. While PRL helps to coordinate osmoregulation [53] and DOM-treated gilts produced more milk during weeks 2 and 3 of lactation [21], there was no apparent effect of late gestational DOM on microvessel density or *AQP* expression at any time in the present study. While microvessel density was unchanged by hyperprolactinemia, the percentage of capillaries in the plexus that were being perfused with blood may have increased [54], augmenting blood flow and nutrient delivery to the MG epithelium [7]. The full relationship between circulating PRL concentrations and vascular permeability in the MG remains to be established.

Hypoxia in the MG is a beneficial event during the transition from gestation to lactation [55, 56], and is evidenced by an increase in the local expression of *HIF-1α* [11]. While others have hypothesized that physiological angiogenesis may be promoted by hypoxia as a means to restore oxygen homeostasis within the MG [12], we did not find changes in *HIF-1α* gene expression within the MG of pigs during this study. Similar to our results, Matmiller *et al.* [57] found no differences in *HIF-1α* gene expression in the bovine MG between 15 days prior to parturition and throughout early lactation. It is possible that HIF-1α can be regulated at both the protein and transcriptional levels [58], but our data does not support a link between altered local *HIF-1α* and *VEGF-A* gene expression and/or microvessel density. This proposal aligns with the previous demonstration that HIF-1α knockout mice undergo MG angiogenesis independently of HIF-1α, and therefore, hypoxia [59].

In conclusion, we have demonstrated that vascular development increases during lactation in the MG of first-parity gilts as evidenced by increased intralobular microvessel density alongside increased overall *VEGF-A* and *AQP* gene expression. We also find that VEGF-A is an epithelium-derived component of the MG secretome. Given that late-gestational hyperprolactinemia had no significant effect on angiogenesis, microvessel density, or *VEGF-A* expression in the porcine MG, further investigation is necessary to establish how DOM imparts its beneficial galactopoietic effect in pigs.

Acknowledgements

This work was supported by a National Research Initiative Competitive Grant 2008-35206-18895 from the USDA National Institute of Food and Agriculture (to RCH), a University of California, Davis College of Agriculture and Environmental Sciences Henry A. Jastro & Peter J. Shields Research Award (to MKVK) and a National Science Foundation Graduate Research Fellowship DGE-0707429 (to MKVK). The authors wish to thank Kent Parker and the UC Davis swine facility for their assistance with the animal work.

References

[1] Neville MC, McFadden TB, Forsyth I. Hormonal regulation of mammary differentiation and milk secretion. J. Mammary Gland Biol. Neoplasia 2002;7:49-66.

[2] Djonov V, Andres AC, Ziemiecki A. Vascular remodelling during the normal and malignant life cycle of the mammary gland. Microsc. Res. Tech. 2001;52:182-189.

[3] Andres AC, Djonov V. The mammary gland vasculature revisited. J. Mammary Gland Biol. Neoplasia 2010;15:319-328.
[4] Geddes DT, Aljazaf KM, Kent JC, Prime DK, Spatz DL, Garbin CP, Lai CT, Hartmann PE. Blood flow characteristics of the human lactating breast. J. Hum. Lact. 2012;28:145-152.
[5] Breen EC. VEGF in biological control. J. Cell Biochem. 2007;102:1358-1367.
[6] Rossiter H, Barresi C, Ghannadan M, Gruber F, Mildner M, Fodinger D, Tschachler E. Inactivation of VEGF in mammary gland epithelium severely compromises mammary gland development and function. FASEB J. 2007;21:3994-4004.
[7] Prosser CG, Davis SR, Farr VC, Lacasse P. Regulation of blood flow in the mammary microvasculature. J. Dairy Sci. 1996;79:1184-1197.
[8] Bruns AF, Bao L, Walker JH, Ponnambalam S. VEGF-A-stimulated signalling in endothelial cells via a dual receptor tyrosine kinase system is dependent on co-ordinated trafficking and proteolysis. Biochem. Soc. Trans. 2009;37:1193-1197.
[9] Staton CA, Kumar I, Reed MW, Brown NJ. Neuropilins in physiological and pathological angiogenesis. J. Pathol. 2007;212:237-248.
[10] Williamson DH, Lund P, Evans RD. Substrate selection and oxygen uptake by the lactating mammary gland. Proc. Nutr. Soc. 1995;54;165-175.
[11] Giordano FJ, Johnson RS. Angiogenesis: the role of the microenvironment in flipping the switch. Curr. Opin. Genet. Dev. 2001;11:35-40.
[12] Bates DO, Harper SJ. Regulation of vascular permeability by vascular endothelial growth factors. Vascul. Pharmacol. 2002;39:225-237.
[13] Nazemi S, Rahbek M, Parhamifar L, Moghimi SM, Babamoradi H, Mehrdana F, Klaerke DA, Knight CH. Reciprocity in the developmental regulation of aquaporins 1, 3 and 5 during pregnancy and lactation in the rat. PLoS One 2014;9:e106809.
[14] Mobasheri A, Barrett-Jolley R. Aquaporin water channels in the mammary gland: from physiology to pathophysiology and neoplasia. J. Mammary Gland Biol. Neoplasia 2014;19;91-102.
[15] Matsuzaki T, Machida N, Tajika Y, Ablimit A, Suzuki T, Aoki T, Hagiwara H, Takata K. Expression and immunolocalization of water-channel aquaporins in the rat and mouse mammary gland. Histochem. Cell Biol. 2005;123:501-512.
[16] Mobasheri A, Kendall BH, Maxwell JE, Sawran AV, German AJ, Marples D, Luck MR, Royal MD. Cellular localization of aquaporins along the secretory pathway of the lactating bovine mammary gland: an immunohistochemical study. Acta. Histochem. 2011;113:137-149.
[17] Clapp C, Thebault S, Martinez De La Escalera G. Role of prolactin and vasoinhibins in the regulation of vascular function in mammary gland. J. Mammary Gland Biol. Neoplasia 2008;13:55-67.
[18] Brisken C, Kaur S, Chavarria TE, Binart N, Sutherland RL, Weinberg RA, Kelly PA, Ormandy CJ. Prolactin controls mammary development via direct and indirect mechanisms. Dev. Biol. 1999;210:96-106.
[19] Trott JF, Schennink A, Petrie WK, Manjarin R, VanKlompenberg M.K, Hovey RC. Triennial Lactation Symposium: Prolactin: The multifaceted potentiator of mammary growth and function. J. Anim. Sci. 2012;90:1674-1686.

[20] Farmer C, Petitclerc D. Specific window of prolactin inhibition in late gestation decreases mammary parenchymal tissue development in gilts. J. Anim. Sci. 2003;81:1823-1829.
[21] VanKlompenberg MK, Manjarin R, Trott JF, McMicking HF, Hovey RC. Late gestational hyperprolactinemia accelerates mammary epithelial cell differentiation that leads to increased milk yield. J. Anim. Sci. 2013;91:1102-1111.
[22] Goldhar AS, Vonderhaar BK, Trott JF, Hovey RC. Prolactin-induced expression of vascular endothelial growth factor via Egr-1. Mol. Cell. Endocrinol. 2005;232:9-19.
[23] Harrell RJ, Thomas MJ, Boyd RD. Limitations of sow milk yield on baby pig growth. Cornell Nutr. Conf., Syracuse NY, 1993; p.156-164.
[24] Horigan KC, Trott JF, Barndollar AS, Scudder JM, Blauwiekel RM, Hovey RC. Hormone interactions confer specific proliferative and histomorphogenic responses in the porcine mammary gland. Domest. Anim. Endocrinol. 2009;37:124-138.
[25] VanKlompenberg MK, McMicking HF, Hovey RC. Technical note: A vacuum-assisted approach for biopsying the mammary glands of various species. J. Dairy Sci. 2012;95:243-246.
[26] Hovey RC, Goldhar AS, Baffi J, Vonderhaar BK. Transcriptional regulation of vascular endothelial growth factor expression in epithelial and stromal cells during mouse mammary gland development. Mol. Endocrinol. 2001;15:819-831.
[27] Barboni B, Turriani M, Galeati G, Spinaci M, Bacci ML, Forni M, Mattioli M. Vascular endothelial groth factor production in growing pig antral follicles. Biol. Reprod. 2000;63:858-864.
[28] Hellerud BC, Nielsen EW, Thorgersen EB, Lindstad JK, Pharo A, Tonnessen TI, Castellheim A, Mollnes TE, Brandtzaeg P. Dissecting the effects of lipopolysaccharides from nonlipopolysaccharide molecules in experimental porcine meningococcal sepsis. Crit. Care Med. 2010;38:1467-1474.
[29] Thorgersen EB, Hellerud BC, Nielsen EW, Barrat-Due A, Fure H, Lindstad JK, Pharo A, Fosse E, Tonnessen TI, Johansen HT, Castellheim A, Mollnes TE. CD14 inhibition efficiently attenuates early inflammatory and hemostatic responses in Escherichia coli sepsis in pigs. FASEB J. 2010;24:712-722.
[30] Larionov A, Krause A, Miller W. A standard curve based method for relative real time PCR data processing. BMC Bioinformatics 2005;6;62.
[31] Yuan JS, Reed A, Chen F, Stewart Jr., CN. Statistical analysis of real-time PCR data. BMC Bioinformatics 2006;7:85.
[32] Piepho HP. Data transformation in statistical analysis of field trials with changing treatment variance. Agron. J. 2009;101:865-869.
[33] Zachary I. Vascular endothelial growth factor. Int. J. Biochem. Cell. Biol. 1998;30:1169-1174.
[34] Pepper MS, Baetens D, Mandriota SJ, Di Sanza C, Oikemus S, Lane TF, Soriano JV, Montesano R, Iruela-Arispe ML. Regulation of VEGF and VEGF receptor expression in the rodent mammary gland during pregnancy, lactation, and involution. Dev. Dyn. 2000;218:507-524.
[35] Hovey RC, McFadden TB, Akers RM. Regulation of mammary gland growth and morphogenesis by the mammary fat pad: a species comparison. J. Mammary Gland Biol. Neoplasia 1999;4:53-68.

[36] Hovey RC, Aimo L. Diverse and active roles for adipocytes during mammary gland growth and function. J Mammary Gland Biol. Neoplasia 2010;15:279-290.
[37] Plein A, Fantin A, Ruhrberg C. Neuropilin regulation of angiogenesis, arteriogenesis, and vascular permeability. Microcirculation 2014;21:315-323.
[38] Kofler NM, Simons M. Angiogenesis versus arteriogenesis: neuropilin modulation of VEGF signaling. F1000Prime Rep. 2015;3:7:26.
[39] Jurisic G, Maby-El Hajjami H, Karaman S, Ochsenbein AM, Alitalo A, Siddiqui SS, Ochoa Pereira C, Petrova TV, Detmar M. An unexpected role of semaphorin3a-neuropilin-1 signaling in lymphatic vessel maturation and valve formation. Circ. Res. 2012;111:426-436.
[40] Fantin A, Vieira JM, Plein A, Denti L, Fruttiger M, Pollard JW, Ruhrberg C. NRP1 acts cell autonomously in endothelium to promote tip cell function during sprouting angiogenesis. Blood 2013;121:2352-2362.
[41] Corbacho AM, Martinez De La Escalera G, Clapp C. Roles of prolactin and related members of the prolactin/growth hormone/placental lactogen family in angiogenesis. J. Endocrinol. 2002;173:219-238.
[42] Struman I, Bentzien F, Lee H, Mainfroid V, D'Angelo G, Goffin V, Weiner RI, Martial JA. Opposing actions of intact and N-terminal fragments of the human prolactin/growth hormone family members on angiogenesis: an efficient mechanism for the regulation of angiogenesis. Proc. Natl. Acad. Sci. 1999;96:1246-1251.
[43] Kobata R, Tsukahara H, Ohshima Y, Ohta N, Tokuriki S, Tamura S, Mayumi M. High levels of growth factors in human breast milk. Early. Hum. Dev. 2008; 84:67-69.
[44] Siafakas CG, Anatolitou F, Fusunyan RD, Walker WA, Sanderson IR. Vascular endothelial growth factor (VEGF) is present in human breast milk and its receptor is present on intestinal epithelial cells. Pediatr. Res. 1999;4:652-657.
[45] Patki S, Patki U, Patil R, Indumathi S, Kaingade P, Bulbule A, Nikam A, Pishte A. Comparison of the levels of the growth factors in umbilical cord serum and human milk and its clinical significance. Cytokine 2012;59:305-308.
[46] Vuorela P, Andersson S, Carpen O, Ylikorkala O, Halmesmaki E. Unbound vascular endothelial growth factor and its receptors in breast, human milk, and newborn intestine. Am. J. Clin. Nutr. 2000;72:1196-1201.
[47] Wagner CL, Taylor SN, Johnson D. Host factors in amniotic fluid and breast milk that contribute to gut maturation. Clin Rev Allergy Immunol. 2008;34:191-204.
[48] Bagnell CA, Steinetz BG, Bartol FF. Milk-borne relaxin and the lactocrine hypothesis for maternal programming of neonatal tissues. Ann. N. Y. Acad. Sci. 2009;1160:152-157.
[49] Bartol FF, Wiley AA, Miller DJ, Silva AJ, Roberts KE, Davolt ML, Chen JC, Frankshun AL, Camp ME, Rahman KM, Vallet JL, Bagnell CA. Lactation Biology Symposium: lactocrine signaling and developmental programming. J. Anim. Sci. 2013;91:696-705.
[50] Blum JW, Baumrucker CR. Colostral and milk insulin-like growth factors and related substances: mammary gland and neonatal (intestinal and systemic) targets. Domest. Anim. Endocrinol. 2002;23:101-110.
[51] Chen JC, Frankshun AL, Wiley AA, Miller DJ, Welch KA, Ho TY, Bartol FF, Bagnell CA. Milk-borne lactocrine-acting factors affect gene expression patterns in the developing neonatal porcine uterus. Reproduction 2011; 141, 675-683.

[52] Curry FR. Microvascular solute and water transport. Microcirculation 2005;12:17-31.
[53] Bole-Feysot C, Goffin V, Edery M, Binart N, Kelly PA. Prolactin (PRL) and its receptor: actions, signal transduction pathways and phenotypes observed in PRL receptor knockout mice. Endocr. Rev. 1998;19:225-268.
[54] Segal SS. Regulation of blood flow in the microcirculation. Microcirculation 2005;12;33-45.
[55] Reynolds M. Mammary respiration in lactating goats. Am. J. Physiol. 1967;212:707-710.
[56] Shao Y, Wellman TL, Lounsbury KM, Zhao FQ. Differential regulation of GLUT1 and GLUT8 expression by hypoxia in mammary epithelial cells. Am. J. Physiol. Regul. Integr. Comp. Physiol. 2014;307:R237-247.
[57] Mattmiller SA, Corl CM, Gandy JC, Loor JJ, Sordillo LM. Glucose transporter and hypoxia-associated gene expression in the mammary gland of transition dairy cattle. J. Dairy Sci. 2011;94:2912-2922.
[58] Kallio PJ, Wilson WJ, O'Brien S, Makino Y, Poellinger L. Regulation of the hypoxia-inducible transcription factor 1alpha by the ubiquitin-proteasome pathway. J. Biol. Chem. 1999;274:6519-6525.
[59] Seagroves TN, Hadsell D, McManaman J, Palmer C, Liao D, McNulty W, Welm B, Wagner KU, Neville M, Johnson RS. HIF1alpha is a critical regulator of secretory differentiation and activation, but not vascular expansion, in the mouse mammary gland. Development 2003;130:1713-1724.

Tables

Table 1. Primers used for qPCR assays. Genes are referred to by protein name.

Accession Number[a]	Gene	Protein	Forward and Reverse Primers (5'-3')	E[b]	T[c]
EU714325.1	*VEGFR-1*	Vascular endothelial growth factor receptor 1	TCCTCCAGAAAGTGCATTCATC TCGCAAATCTTCACCACGTT	112	60
EU714326.1	*VEGFR-2*	Vascular endothelial growth factor receptor 2	TGGAATTGACAAGACAGCAACTT CTCGGTGTTCGCTGTGTGTT	101	60
XM_003130798.1	*NP1*	Neuropilin 1	CTGCCACAGCGGAACAGG CGTTGGAAACTCTGATTGTATAGTGCT	94	60

NM_ 001123124.1	*HIF1a*	Hypoxia inducible factor 1 alpha	GAGTTCACCTGAGCCTAACAGTCCC CAGCAAAAAGTTTCTCTACCAATTCCAAC	97	62
NM_ 214454.1	*AQP1*	Aquaporin 1	GCCATCGGCTTCTCTGTGG GGTCCTGGAAGTTGTGCGTG	89	60
NM_ 001110172.1	*AQP3*	Aquaporin 3	CTCTGGCTATGCCGTCAACC CAGGAGCGGAGAGACAATGG	87	60

[a]Accession number corresponds to the cDNA or the expressed sequence tag sequence deposited in the GenBank database.

[b]Primer pair efficiency (%). All reference and target gene standard curves had an $R^2 > 0.98$.

[c]Annealing temperature (°C) used for each primer pair.

Table 2. Vascular endothelial growth factor A (VEGF-A) isoform primers used for qPCR assays.

Isoform	Forward and Reverse Primers (5'-3')	E[a]	T[b]	Location[c] (Exon)
VEGF-A$_{120}$	CATGCAGATTATGCGGATCAA GGCTTGTCACATTTTTCTTGC	112	60	3-4 5-8a
VEGF-A$_{144}$	GCGAGGCAAGAAAAAAATCAGTT GCTTGTCACATACGCTCCAGG	110	60	5-6a 6a-8a

VEGF-A$_{147}$	TCGGAGCGGAGAAAGCATT GTCACATCTTGCAACGCGAG	93	60	7a 7a-8a
VEGF-A$_{164}$	GATAGAGCGAGGCAAGAAAATCC TCACATCTGCAAGTACGTTCGTTT	91	60	5-7a 7b-8a
VEGF-A$_{164}$*b*	ATAGAGCGAGGCAAGAAAATCCC TCCTGGTGAGACGTCTGCAAGTAC	96	64	5-7a 7b-8b
VEGF-A$_{182}$	GCAAGAAATCCCTCCCTGTGG[d] GTCTGGTGCCCAAAACGCTG	101	62	6a(short)-7a 8a-8b
VEGF-A$_{188}$	CTGGAGCGTTCCCTGTGG TCAAGCTGCCTCGCCTTG	95	60	6a-7a 7a-7b

[a]Primer pair efficiency (%). All reference and target gene standard curves had an $R^2 > 0.97$.

[b]Annealing temperature (°C) used for each primer pair.

[c]Location of the primer within the VEGF-A gene

[d]The correct sequence for this primer should be GCAAGAAATCCC**G**TCCCTGTGG. The bold G is different from the VEGF-A_{182} forward primer actually used. Validation experiments confirmed that the efficiency of amplification was not affected by the one bp deletion.

Figure Legends

Figure 1. Microvessel density in the porcine mammary gland (MG) during late gestation and lactation. (A) Representative images showing immunohistochemistry for CD31 from a control (CON) animal. Arrowheads point to an example of a positively stained vessel (brown staining). Negative control is a representative section incubated with secondary antibody alone. Scale bar is 100 microns. (B) The density of microvessels within the MG was expressed as the number of cross-sectioned microvessels per unit area of intralobular stroma (calculated by subtracting the

569 alveolar area from the corresponding total lobular area) for untreated (CON, solid bars) and
570 domperidone (DOM)-treated females (open bars). Data are the mean number of CD31-positive
571 vessels per unit of intralobular area ± SEM (n = 3-6); *$P < 0.05$.

572

573 Figure 2. Expression of vascular endothelial growth factor A (*VEGF-A*) isoforms in the porcine
574 mammary gland during gestation and lactation. Quantitative PCR was used to quantify the
575 relative mRNA abundance of A) *VEGF-A*$_{120}$, B) *VEGF-A*$_{144}$, C) *VEGF-A*$_{147}$, D) *VEGF-A*$_{164}$, E)
576 *VEGF-A*$_{164}$*b*, F) *VEGF-A*$_{182}$, and G) *VEGF-A*$_{188}$ in mammary tissue of either untreated (CON,
577 solid bars) or domperidone-treated (DOM, open bars) gilts. Data are means ± SEM (n = 3-6);
578 *$P< 0.05$, **$P< 0.01$.

579

580 Figure 3. Concentration of vascular endothelial growth factor A (VEGF-A) in colostrum
581 (Colost.)/milk and plasma from untreated (CON, solid bars) and domperidone-treated (DOM,
582 open bars) gilts during early and late lactation. In early lactation, colostrum was collected on day
583 1 of lactation while plasma was collected on day 2. In late lactation, milk was collected on day
584 20 while plasma was collected on day 21. Data are arithmetic means ± SEM (n = 3); ***$P<$
585 0.001.

586

587 Figure 4. Immunohistochemical localization of vascular endothelial growth factor A (VEGF-A)
588 in the mammary glands of gilts during late gestation and lactation. Images are representative of
589 all animals. Arrowheads point to regions of immunoreactivity evidenced by dark blue staining

590 using the Vector SG chromogen. Negative control is a representative section incubated with
591 secondary antibody alone. Scale bar is 50 microns.

592

593 Figure 5. Abundance of mRNA encoding receptors for vascular endothelial growth factor A.
594 Quantitative PCR was used to quantify the relative mRNA abundance for A) vascular endothelial
595 growth factor receptor 1 (*VEGFR-1*), B) vascular endothelial growth factor receptor 2 (*VEGFR-*
596 *2*), and C) neuropilin 1 (*NP1*) in the mammary glands during gestation and lactation. Gilts were
597 either untreated (CON, solid bars) or received domperidone (DOM, open bars) from days 90 to
598 110 of gestation. Data are means ± SEM (n = 3-6); **P*< 0.05.

599

600 Figure 6. Gene expression for aquaporins in the porcine mammary gland during gestation and
601 lactation. Quantitative PCR was used to quantify the relative mRNA abundance for A) aquaporin
602 1 (*AQP1*) and B) aquaporin 3 (*AQP3*) in the mammary glands of gilts that were either untreated
603 (CON, solid bars) or received domperidone (DOM, open bars) from days 90 to 110 of gestation.
604 Data are means ± SEM (n = 3-6); **P*< 0.05, ****P*< 0.001.

Figure 1

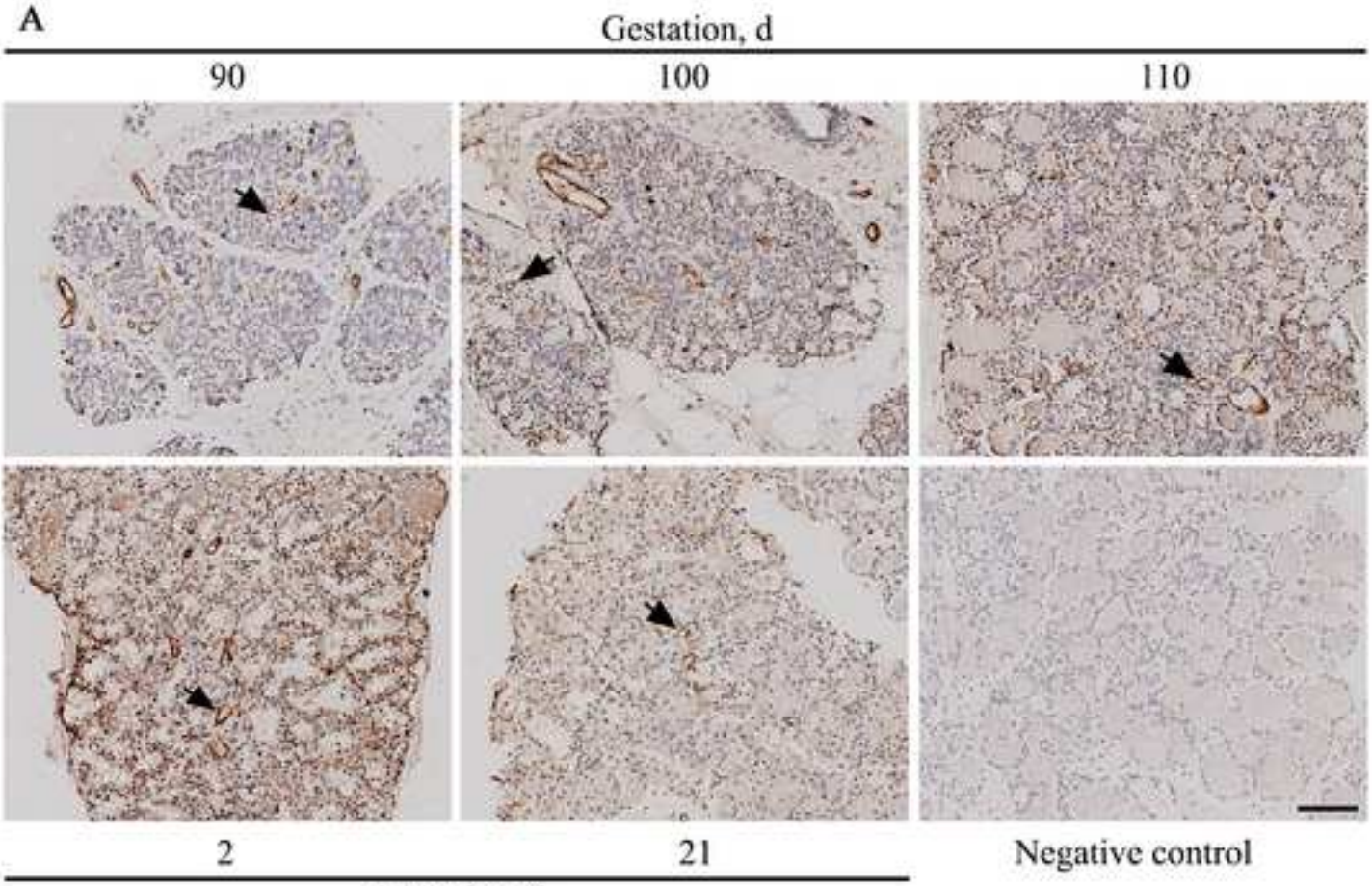
A
Gestation, d
90
100
110
2
21
Negative control
Lactation, d

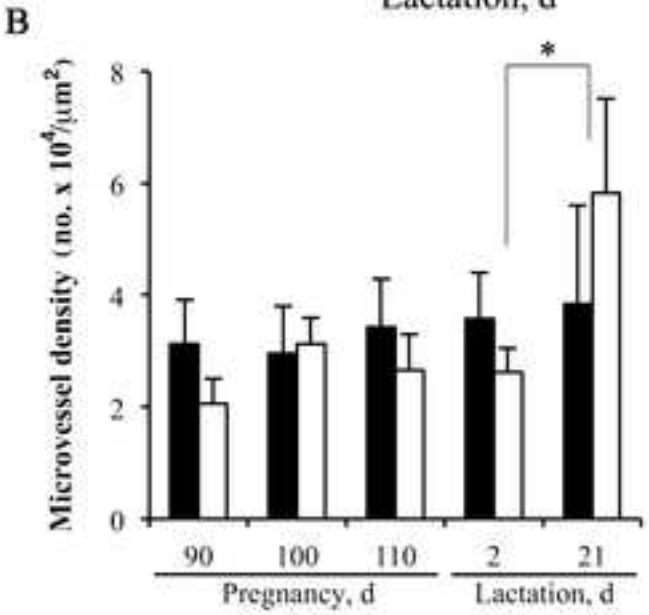
B
Microvessel density (no. x 10⁴/μm²)
0
2
4
6
8
*
90
100
110
2
21
Pregnancy, d
Lactation, d

Figure 2

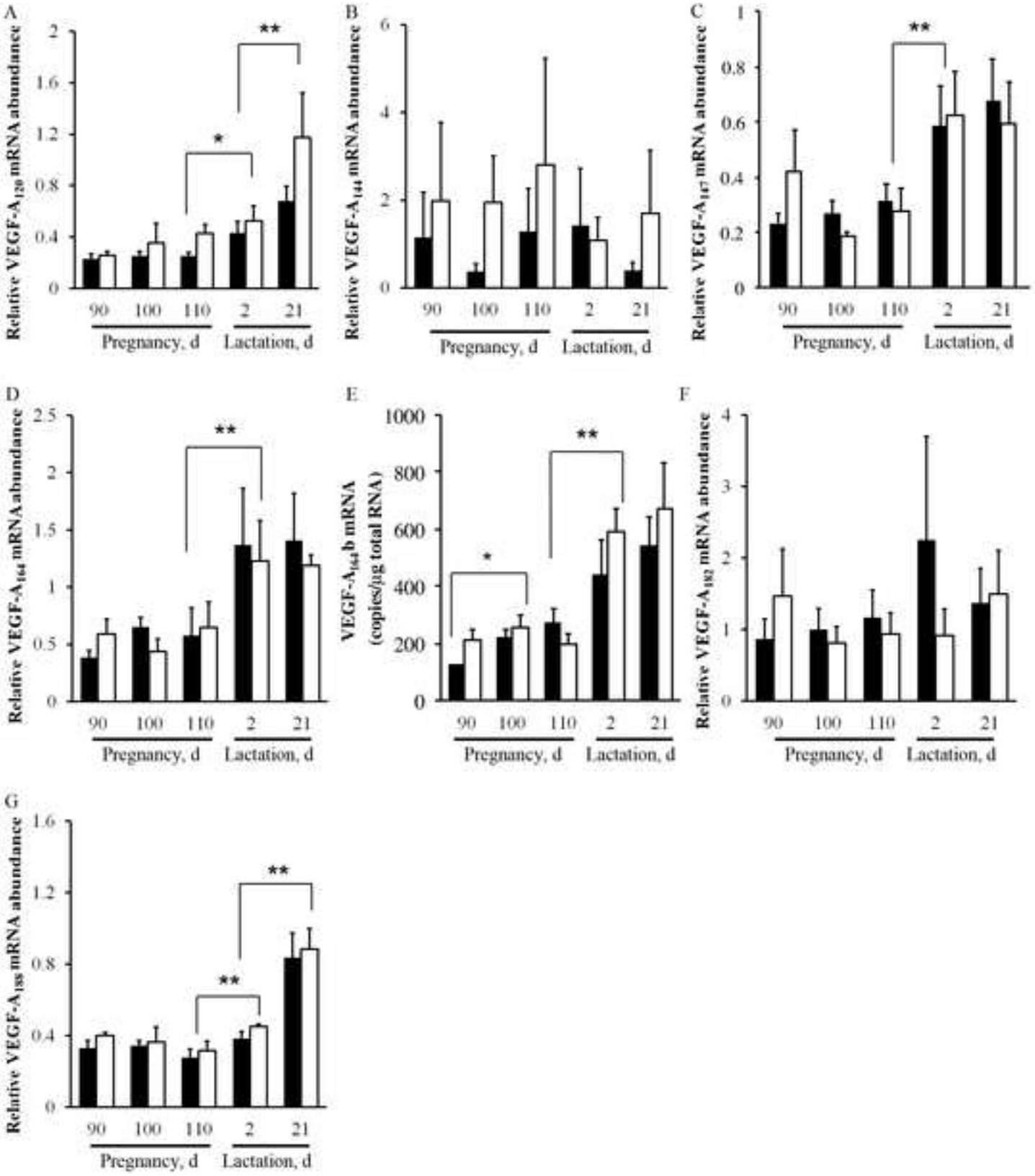
A
Relative VEGF-A120 mRNA abundance
2
1.6
1.2
0.8
0.4
0
*
**
90
100
110
2
21
Pregnancy, d
Lactation, d
B
Relative VEGF-A144 mRNA abundance
6
4
2
0
90
100
110
2
21
Pregnancy, d
Lactation, d
C
Relative VEGF-A147 mRNA abundance
1
0.8
0.6
0.4
0.2
0
**
90
100
110
2
21
Pregnancy, d
Lactation, d
D
Relative VEGF-A164 mRNA abundance
2.5
2
1.5
1
0.5
0
**
90
100
110
2
21
Pregnancy, d
Lactation, d
E
VEGF-A164b mRNA (copies/μg total RNA)
1000
800
600
400
200
0
*
**
90
100
110
2
21
Pregnancy, d
Lactation, d
F
Relative VEGF-A182 mRNA abundance
4
3
2
1
0
90
100
110
2
21
Pregnancy, d
Lactation, d
G
Relative VEGF-A188 mRNA abundance
1.6
1.2
0.8
0.4
0
**
**
90
100
110
2
21
Pregnancy, d
Lactation, d

Figure 3

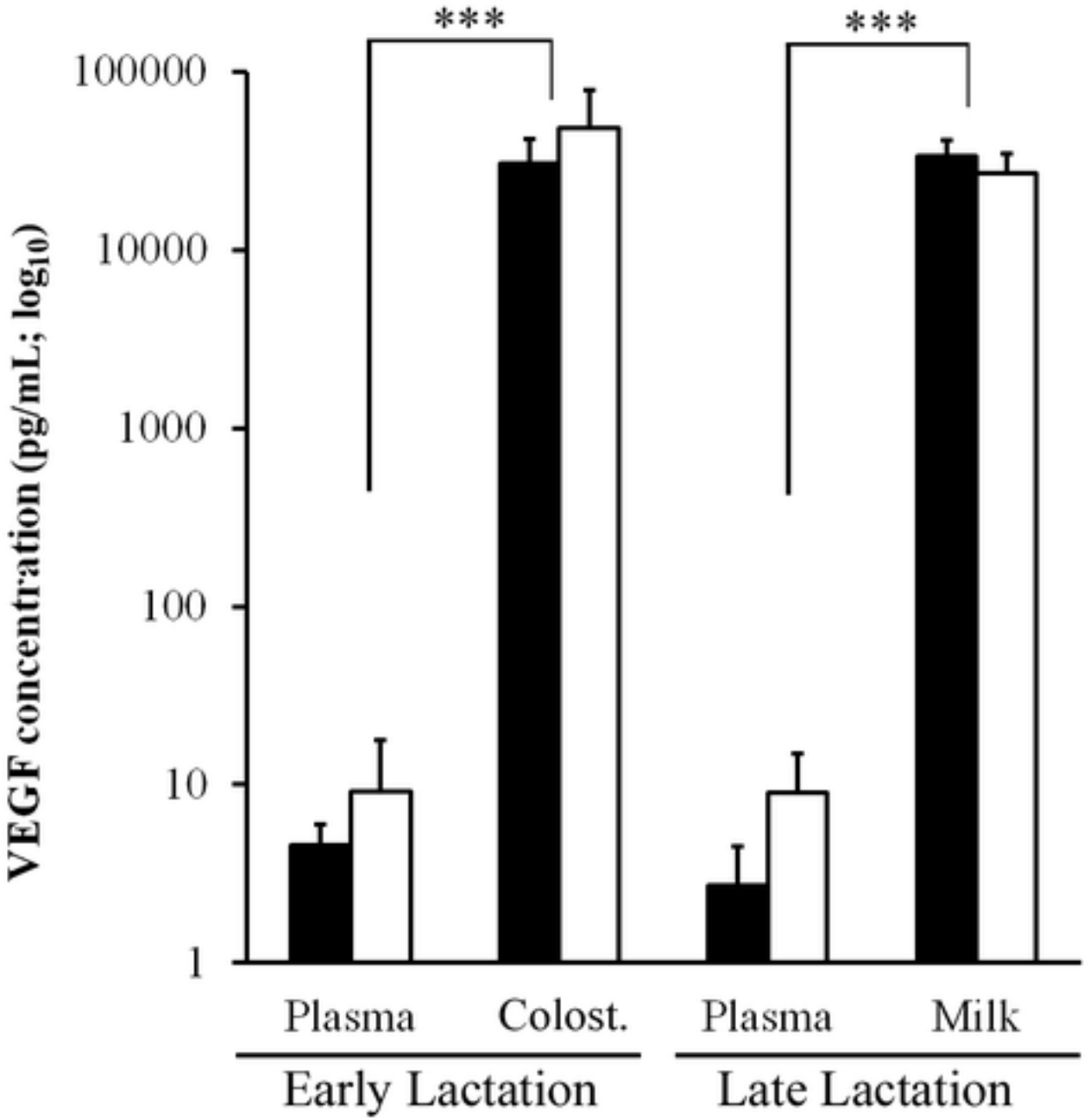
***
***
100000
10000
1000
100
10
1
VEGF concentration (pg/mL; log10)
Plasma
Colost.
Plasma
Milk
Early Lactation
Late Lactation

Figure 4

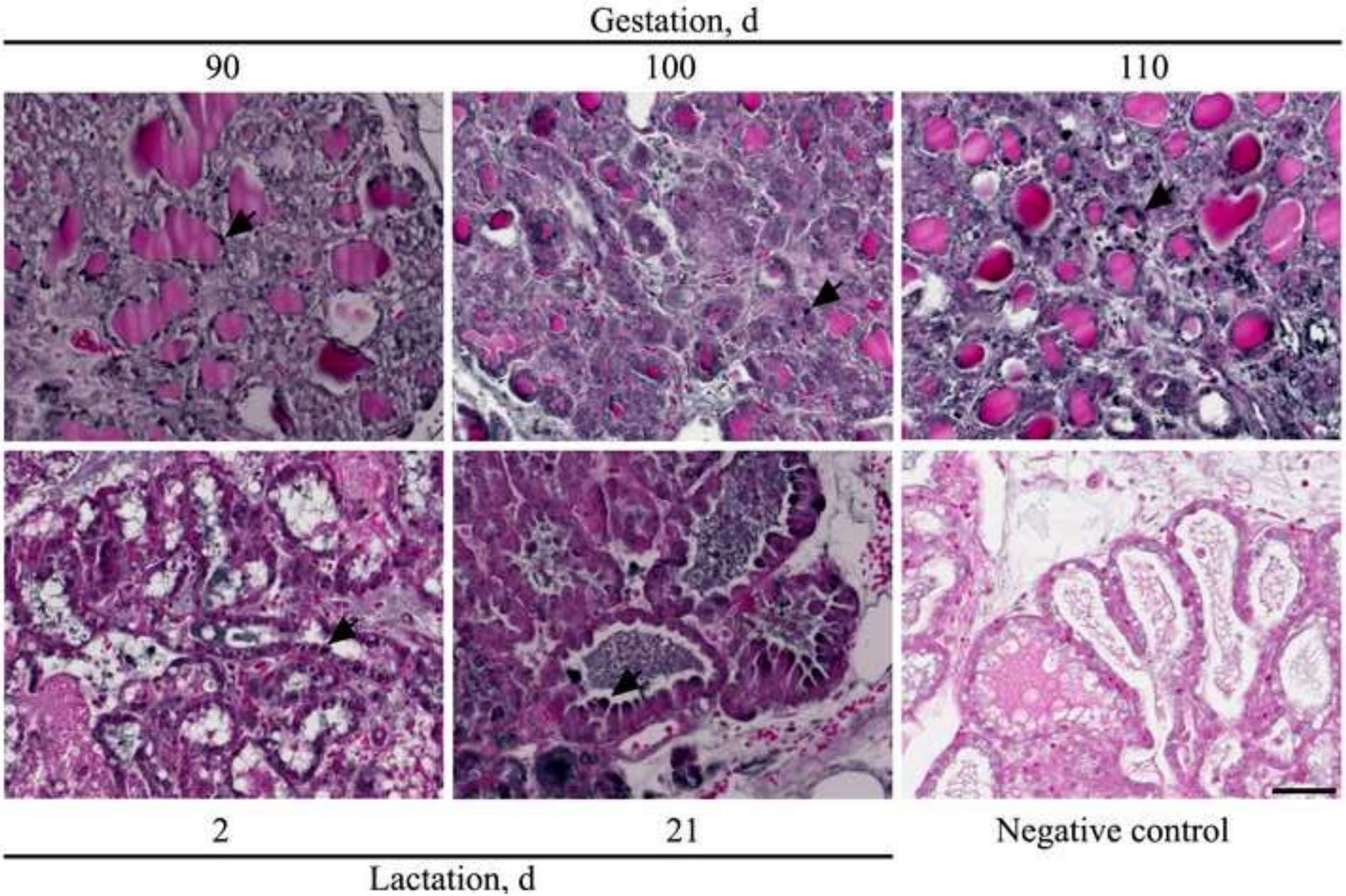

Figure 5

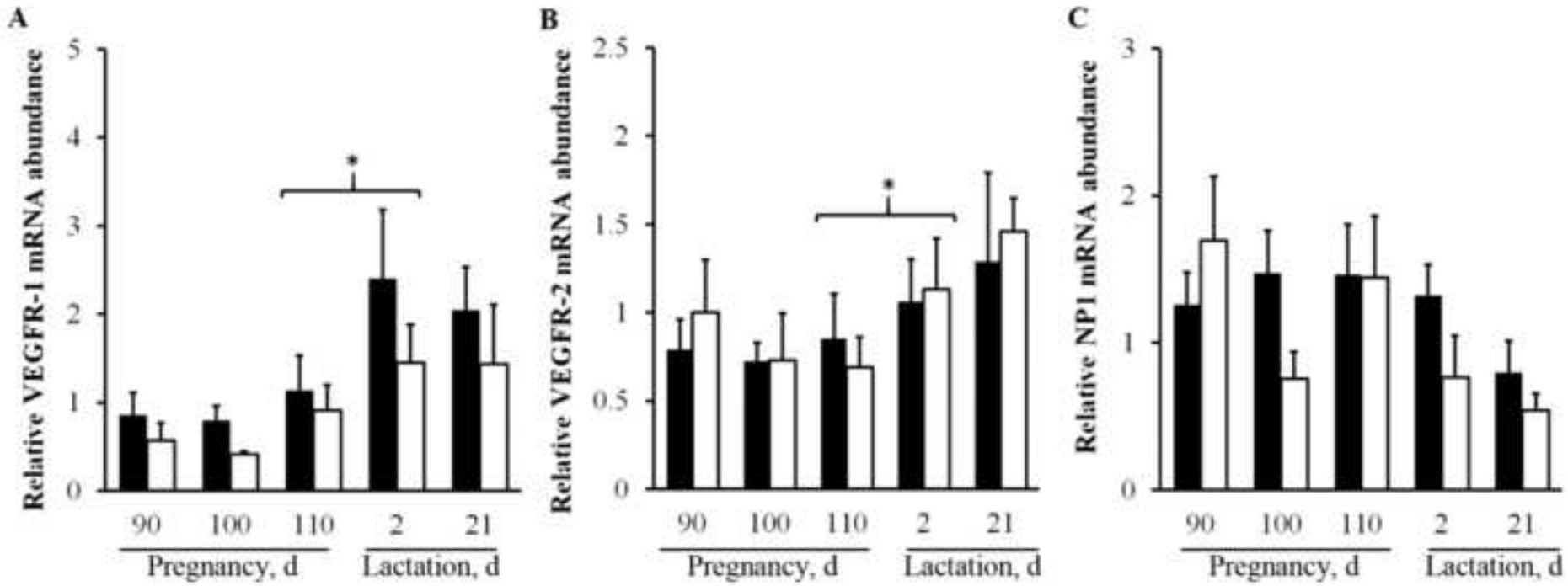
A
Relative VEGFR-1 mRNA abundance
0
1
2
3
4
5
*
90
100
110
2
21
Pregnancy, d
Lactation, d
B
Relative VEGFR-2 mRNA abundance
0
0.5
1
1.5
2
2.5
*
90
100
110
2
21
Pregnancy, d
Lactation, d
C
Relative NP1 mRNA abundance
0
1
2
3
90
100
110
2
21
Pregnancy, d
Lactation, d

Figure 6

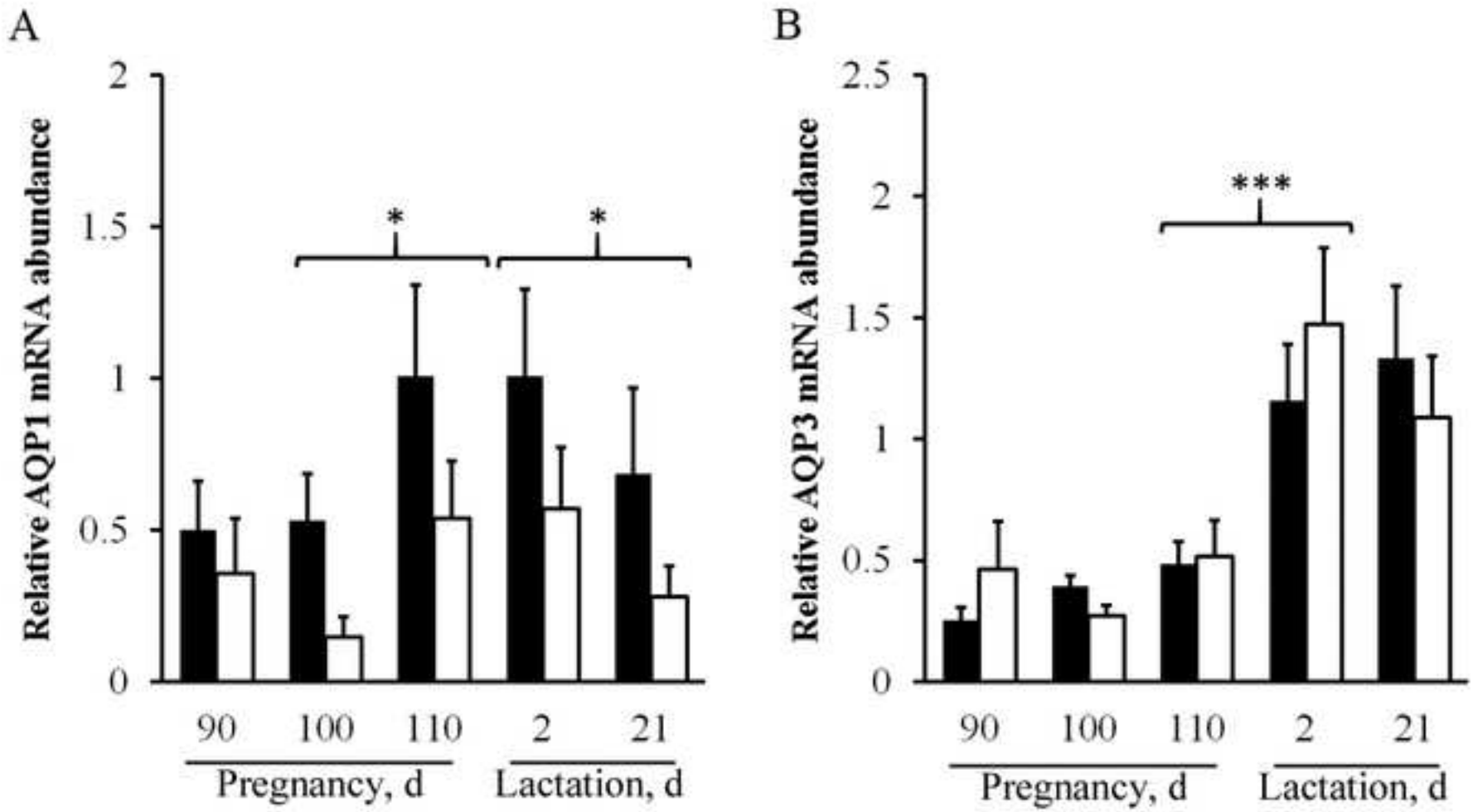
A
Relative AQP1 mRNA abundance
2
1.5
1
0.5
0
*
*
90
100
110
2
21
Pregnancy, d
Lactation, d
B
Relative AQP3 mRNA abundance
2.5
2
1.5
1
0.5
0
***
90
100
110
2
21
Pregnancy, d
Lactation, d